Accepted Manuscript

Neural network adaptive sliding mode control for omnidirectional vehicle with uncertainties

xingyang lu, Xiangyin Zhang, Guoliang Zhang, Jinhui Fan, Songmin Jia

PII: S0019-0578(18)30422-1
DOI: https://doi.org/10.1016/j.isatra.2018.10.043
Reference: ISATRA 2944

To appear in: *ISA Transactions*

Received date : 25 June 2018
Revised date : 14 September 2018
Accepted date : 26 October 2018

Please cite this article as: lu x., et al. Neural network adaptive sliding mode control for omnidirectional vehicle with uncertainties. *ISA Transactions* (2018), https://doi.org/10.1016/j.isatra.2018.10.043

Xingyang Lu, Xiangyin Zhang, Guoliang Zhang, Jinhui Fan, Songmin Jia

[1] *Faulty of Information Technology, Beijing University of Technology, Beijing, China*

[2] *Beijing Key Laboratory of Computational Intelligence and Intelligent System, Beijing, China*

[3] *Engineering Research Center of Digital Community, Ministry of Education, Beijing, China*

Graphical Ab

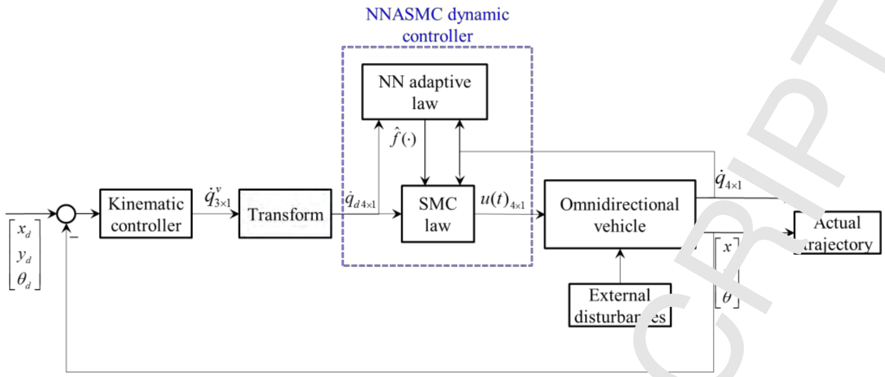

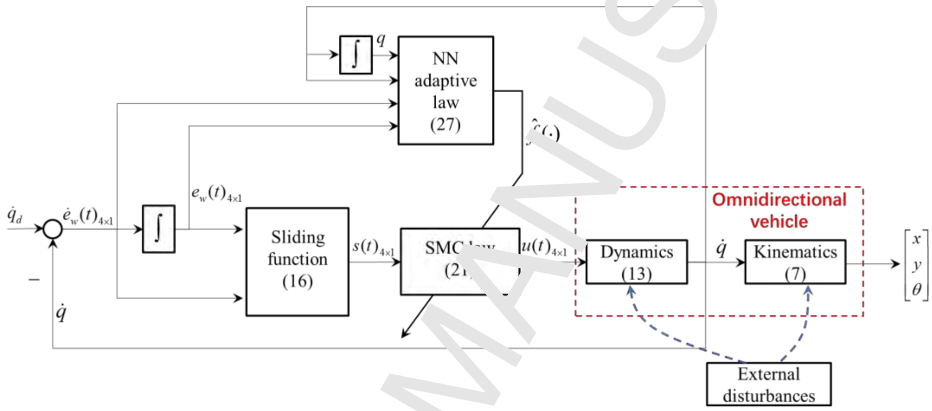

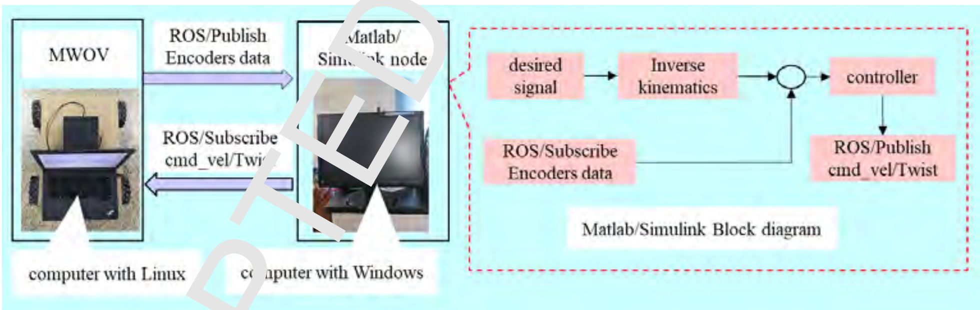

Highlights

1. This paper presents a novel neural network adaptive sliding mode control (NNASMC) method for the dynamic controller design of an omnidirectional vehicle.
2. Kinematic and dynamic modeling of the omnidirectional vehicle is presented with uncertainties and unknown external disturbances.
3. Artificial neural network (ANN) based adaptive law is introduced to model and estimated the various uncertainties disturbances.
4. The performance of the proposed NNASMC method is verified through computer simulations and physical experiments on the omnidirectional vehicle plantform.
5. Results validate the effectiveness and robustness of the NNASMC method in presence of uncertainties and unknown external disturbances.

Neural Network Adaptive Sliding Mode Control for Omnidirectional Vehicle with Uncertainties

Abstract:

This paper presents a novel neural network adaptive sliding mode control (NNASMC) method to design the dynamic control system for an omnidirectional vehicle. The omnidirectional vehicle is equipped with four Mecanum wheels that are actuated by separate motors, and thus has the omnidirectional mobility and excellent athletic ability in a narrow space. Considering various uncertainties and unknown external disturbances, kinematic and dynamic models of the omnidirectional vehicle are established. The inner-loop controller is designed based the sliding mode control (SMC) method, while the out-loop controller uses the proportion integral derivative (PID) method. In order to achieve the stable and robust performance, the artificial neural network (ANN) based adaptive law is introduced to model and estimated the various uncertainties disturbances. Stability and robustness of the proposed control method are analyzed using the Lyapunov theory. The performance of the proposed NNASMC method is verified and compared with the classical PID controller and SMC controller through both the computer simulation and the platform experiment. Results validate the effectiveness and robustness of the NNASMC method in presence of uncertainties and unknown external disturbances.

Keywords: omnidirectional vehicle, sliding mode control, Mecanum wheel, artificial neural network.

1. Introduction

Omnidirectional vehicles can perform translational and rotational motion independently and simultaneously. Therefore, omnidirectional vehicles are being been widely used on various occasions, especially those in narrow spaces, such as hospitals, factories and sheltered workshops for disabled people. The Mecanum wheel omnidirectional vehicles (MWOV) is common example of mobile vehicles with the omnidirectional ability [1-3]. The Mecanum wheel consists a series of passive rollers, which are mounted at 45° angle around its hub circumference, is a special kind of wheels that can allow the lateral movement without changing attitude of the wheel itself [4-7]. Owning to the sidesway characteristic of Mecanum wheels, the MWOV can move to any position without changing its orientation, which is different from conventional vehicles. In particular, the MWOV has the outstanding flexibility and maneuverability of movement in the narrow workspace, and thus, it has been effectively and efficiently applied to logistics sorting factory, soccer robots, hospitals, military, home applications and so on [8-10]. Research on MWOVs is so popular around the world, especially the vehicle that is equipped with four Mecanum wheels [1-3] [11-12]. In the four Mecanum wheels vehicle, the four wheels are arranged symmetrically on the geometric center of the vehicle, and four separate motors drives the four wheels respectively.

Due to the coordination and cooperation of the four individual motors as well as the various uncertainties in the real world, the high-precision motion control of the MWOV is a challenging issue for researchers. Various control algorithms [13-19] were applied to the motion control of the robot during past decades, including sliding mode control (SMC), robust control, adaptive control, disturbances observer-based control, and so on. Chen et al. [13] presented an adaptive sliding-mode dynamic controller for asymptotically stabilizing the non-holonomic mobile robot to a desired trajectory without considering the uncertainties. Miao et al. [14] proposed a novel adaptive neural network controller for trajectory tracking of autonomous underwater vehicle, which employing radial basic function neural network to account for modeling errors. Kim et al. [15] designed a robust adaptive controller to overcome uncertainties and external disturbances for the mobile robot under non-holonomic constraints can achieve perfect velocity tracking. Purwin and Andrea [16] proposed an algorithm to generate a trajectory and optimal control for four wheeled omnidirectional vehicles under limited friction condition. However, most of the above control methods depend on the modelling accuracy of the vehicle, and thus, cannot have a satisfactory handle on the model uncertainties and unknown external disturbances well, especially on the Mecanum wheel vehicle.

The SMC is one of the effective approaches that can theoretically achieve the perfect control performance of the nonlinear dynamic system with model uncertainties [20-22]. Ashrafiuon et al. [20] presented a sliding mode tracking controller for trajectory tracking of autonomous surface vessels, which uses two sliding surfaces for surge tracking errors and lateral motion tracking errors. Qian et al [21] developed a robust control method that combined SMC and the nonlinear disturbances observer for formation maneuvers of a multi-agent system with uncertainties. Ferrara and Incremona [22] proposed an integral suboptimal second-order SMC algorithm for robot manipulators to solve motion control problems.

Actually, considering that uncertainties and external disturbances often exist in the omnidirectional motion system, it is necessary to design an adaptive law to help the SMC method improve the robustness. In particular, for the MWOV system, the dynamic changing uncertainties have the serious impact on the vehicle, for instance, cause the vehicle to deviate from its desired trajectory. In [23], an adaptive SMC controller based on dynamic structure fuzzy wavelet neural networks was proposed for industrial robot manipulator control system with uncertainties and disturbances. In [24], a novel adaptive tracking controller based on neural networks is proposed for mobile robots to implement the trajectory tracking mission. In [25], an adaptive SMC method was applied to a three wheel omnidirectional mobile robot with both structured and unstructured uncertainties. Yang et al. [26] proposed a control scheme based Radial Basis Function (RBF) neural network to learn the unknown robot manipulators dynamics.

Motivated by these previous work about SMC and adaptive control methods, a neural network adaptive sliding mode control (NNASMC) method for dynamic control of the MWOV system with modeling uncertainties and unknown external disturbances is derived in this paper. The approximation ability of artificial neural networks is employed to estimate the various uncertainties in the model. Stability and robustness of the proposed control method are analyzed using the Lyapunov theory. The performance of the proposed NNASMC method is verified and compared with the classical proportion integral derivative (PID) controller and SMC controller through computer simulations and platform experiments on the omnidirectional vehicle. Results validate the effectiveness and robustness of the NNASMC method in presence of uncertainties and unknown external disturbances.

The rest of this article is organized as follows. In Section 2, kinematics and dynamics of the omnidirectional vehicle with uncertainties are modeled. Section 3 presents the proposed control scheme in detail, which is followed by the stability analysis in Section 4. Simulation and experimental results are given in Section 5 and Section 6 respectively. Finally, the conclusion is given in Section 7.

2. Model Description

Kinematics depicts the mathematical relationship between the position and velocity of the vehicle, while dynamics can clearly describe the role of the force on the position and speed of the vehicle. In this section, the kinematic model and the dynamic model are presented for the omnidirectional vehicle equipped with four Mecanum wheels (as is shown in Fig. 1), which considering model uncertainties and unknown external disturbances [1-3], [27-28].

2.1. Kinematics

As is shown in Fig. 1, in the MWOV, four wheels are arranged symmetrically on the geometric center of the vehicle body to achieve the uniform load of each wheel and the stability of supporting structure. Each wheel is driven by a DC motor independently to produce the torque required for the motion of the vehicle. Due to the geometric characteristics of the Mecanum wheel, the robot can achieve omnidirectional motion on the platform through appropriate combination of speeds of the four wheels. For the derivation of the equation of motion, we have the following two assumptions.

Assumption 1 The vehicle moves on the horizontal plane and the plane.

Assumption 2 All the components of the vehicle, including wheels, are rigid.

In Fig. 1, three coordinate frames are established, including the fixed coordinate frame O, the vehicle moving coordinate frame O_r, and the wheel coordinate frame O_i^w (i = 1, 2, 3, 4). The point O_r is the gravity center of the vehicle.

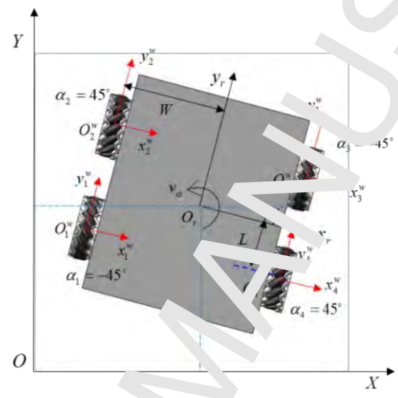

Fig.1 Kinematic geometry of a MWOV

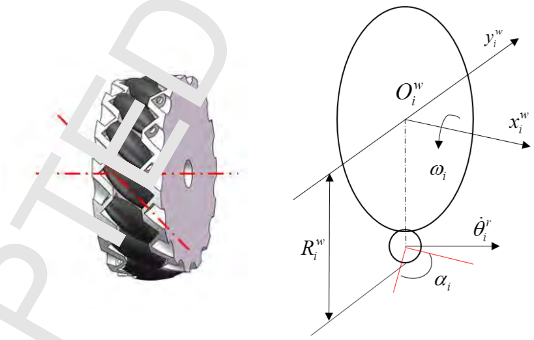

Fig.2 Structure sketch of the Mecanum wheel

The inverse kinematics model and kinematics model of the mobile vehicle as shown in Fig. 1 is given as follows:

$$\begin{bmatrix} \omega_1 \\ \omega_2 \\ \omega_3 \\ \omega_4 \end{bmatrix} = \frac{1}{R} \begin{bmatrix} -1 & 1 & -(L+W) \\ 1 & 1 & -(L+W) \\ -1 & 1 & L+W \\ 1 & 1 & L+W \end{bmatrix} \begin{bmatrix} v_x \\ v_y \\ v_\omega \end{bmatrix} \tag{1}$$

$$\begin{bmatrix} v_x \\ v_y \\ v_\omega \end{bmatrix} = \frac{R}{4}\begin{bmatrix} -1 & 1 & -1 & 1 \\ 1 & 1 & 1 & 1 \\ -\frac{1}{L+W} & -\frac{1}{L+W} & \frac{1}{L+W} & \frac{1}{L+W} \end{bmatrix}\begin{bmatrix} \omega_1 \\ \omega_2 \\ \omega_3 \\ \omega_4 \end{bmatrix} \tag{2}$$

where ω_i (i=1, 2, 3, 4) is the wheel angular velocity around the hub, $\dot{q}^v=\begin{bmatrix} v_x & v_y & v_\omega \end{bmatrix}^T$ is the velocity vector of wheel in coordinate frame O, W and L are translational distance between O_r and O_i^w in x and y direction respectively and R is the wheel radius.

2.2. Dynamics

The MWOV with uncertainties moving on a plane flat surface is developed using Lagrange method. In order to derive the equation of motion, the following assumptions are considered.

Assumption 3 The moving coordinate frame O lies on the center of gravity of the vehicle.

Assumption 4 The vehicle moves on a planar surface and its potential energy is kept constant, where the potential energy is zero.

Assumption 5 Neglecting the inertia of rollers of the Mecanum.

Using the Lagrange method the dynamics is obtained as:

$$M(q)\ddot{q} + D_w(q)\dot{q} = u(t) - \tau_d \tag{3}$$

where D_w is the coefficient of the wheel's viscous friction, $u(t)=[u_1(t) \quad u_2(t) \quad u_3(t) \quad u_4(t)]^T$, $u_i(t)(i=1,2,3,4)$ represents the control input of each wheel, τ_d represents external disturbances, $\dot{q}=[\omega_1 \quad \omega_2 \quad \omega_3 \quad \omega_4]^T$ is the angular velocity of the Mecanum wheel. Considering the parameter variations in the vehicle, the positive definite system inertia matrix $M(q)$ can be respectively expressed as $M(q) = M_0(q) + \Delta M$, while the coefficient of the wheel's viscous friction $D_w(q)$ can be expressed as $D_w(q) = D_w^0(q) + \Delta D_w$, where ΔM and ΔD_w are the perturbed terms, $M_0(q)$ and $D_w^0(q)$ are the nominal values. Hence, the dynamic model of the vehicle is as follows:

$$(M_0(q) + \Delta M)\ddot{q} + (D_w^0(q) + \Delta D_w)\dot{q} = u(t) - \tau_d \tag{4}$$

Therefore,

$$M_0(q)\ddot{q} + D_w^0(q)\dot{q} = u(t) - \tau_d - \Delta M\ddot{q} - \Delta D_w\dot{q} = u(t) - E(q) \tag{5}$$

Where $M_0(q)=\begin{bmatrix} A+B+I_\omega & -B & B & A-B \\ -B & A+B+I_\omega & A-B & B \\ B & A-B & A+B+I_\omega & -B \\ A-B & B & -B & A+B+I_\omega \end{bmatrix}$, $A=mR^2/8$, $B=I_zR^2/16(W+L)^2$

, $D_w^0(q)=[D_{w1}^0 \quad D_{w2}^0 \quad D_{w3}^0 \quad D_{w4}^0]^T$, $E(q)=\tau_d+\Delta M\ddot{q}+\Delta D_w\dot{q}$, and $E(q)$ is the function about the model uncertainties and the external disturbances, m is the total mass of the vehicle, and I_z, I_ω denote the moment of inertia of the vehicle's body and the wheels, respectively.

3. Methodology

In this section, a stability controller based on NNASMC is designed to enable the omnidirectional vehicle to track the desired trajectory in presence of uncertainties and unknown external disturbances. The designed control scheme is divided into two parts, namely the kinematics controller for the outer-loop and the dynamic controller for the inner-loop, which can be seen in Fig. 3. The outer-loop controller adopts the classical proportion integral derivative (PID) control method. In the inner loop, the NNASMC is proposed to achieve the stable and robust performance, as is shown in Fig. 4.

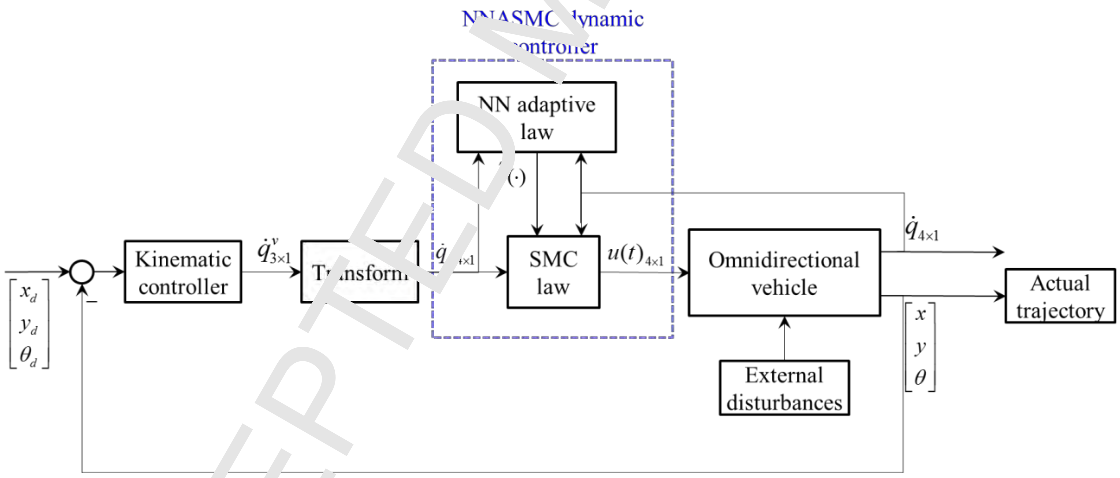

Fig.3 Diagram of the control system

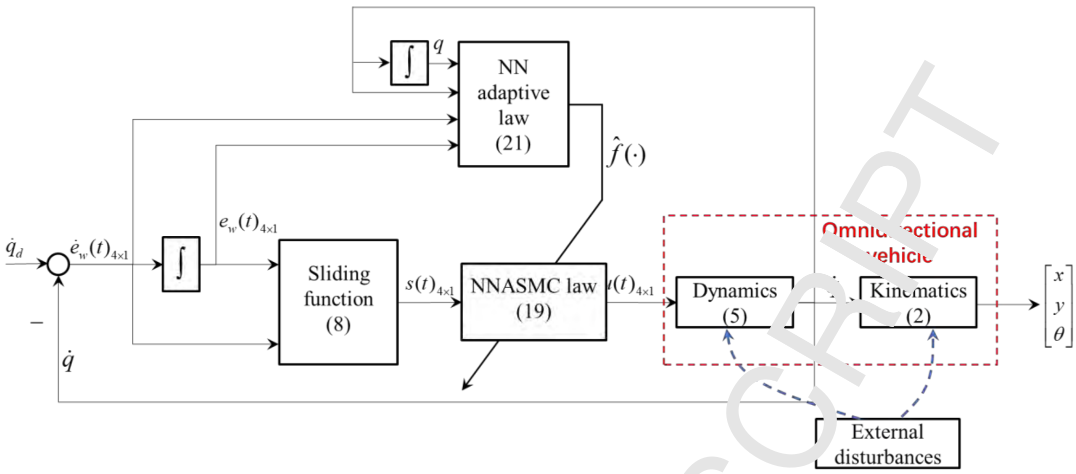

Fig.4 Diagram of the inner-loop controller based on NNASMC

3.1. SMC law

The SMC method is utilized to design a dynamic tracking controller in this subsection, so that the actual position of the wheel converges to the control position. Because the sliding mode control algorithm is strongly dependent on the model, the design of sliding mode control law first assumes that there is no uncertainty in the system model, that is, the system parameters are known, and the disturbance is zero. Before designing the SMC controller, the dynamic model of the vehicle is rewritten as follows:

$$\begin{aligned}\ddot{q} &= M_0^{-1}(q)(u(t) - E(q) - D_w^0(q)\dot{q}) \\ &= M_0^{-1}(q)u(t) - M_0^{-1}(q)E(q) - M_0^{-1}(q)D_w^0(q)\dot{q} \\ &= M_0^{-1}(q)u(t) - M_0^{-1}(q)E(q) - H_0(q)\dot{q}\end{aligned} \tag{6}$$

where define the function of $g(q) = M_0^{-1}(q)E(q)$ and suppose that the uncertainty $g(q)$ is zero. Then, the following equation is obtained:

$$\ddot{q} = M_0^{-1}(q)u(t) - H_0(q)\dot{q} \tag{7}$$

The control objective is to make the actual position q of the wheel follow the reference position q_d precisely, that is, the tracking error $e_w(t)_{4\times1} = q_d - q$ is as close to zero as possible. To achieve precise and fast control objective, the following sliding surface is defined as:

$$s(t)_{4\times1} = \dot{e}_w(t)_{4\times1} + \Lambda_{4\times4} e_w(t)_{4\times1} \tag{8}$$

where $e_w(t)_{4\times1} = \left[e_1^w(t) \quad e_2^w(t) \quad e_3^w(t) \quad e_4^w(t) \right]^T$ and $\Lambda_{4\times4} = diag(\lambda_1 \quad \lambda_2 \quad \lambda_3 \quad \lambda_4)$ is a design constant positive matrix. Differentiating the above sliding-surface variable with respect to time t, the following equation is obtained:

$$\begin{aligned} \dot{s}(t)_{4\times1} &= \ddot{e}_w(t)_{4\times1} + \Lambda_{4\times4}\dot{e}_w(t)_{4\times1} \\ &= \ddot{q}_d - \ddot{q} + \Lambda_{4\times4}\dot{e}_w(t)_{4\times1} \\ &= \ddot{q}_d + \Lambda_{4\times4}\dot{e}_w(t)_{4\times1} - M_0^{-1}(q)u(t) + H_0(q)\dot{q} \end{aligned} \tag{9}$$

Here, the following reaching law is adopted:

$$\dot{s}(t)_{4\times1} = -k_{4\times4}^{s1} s(t)_{4\times1} - k_{4\times4}^{s2}\,\text{sgn}(s(t)_{4\times1}) \tag{10}$$

where $k_{4\times4}^{s1} = diag(k_1^{s1} \quad k_2^{s1} \quad k_3^{s1} \quad k_4^{s1})$, $k_{4\times4}^{s2} = diag(k_1^{s2} \quad k_2^{s2} \quad k_3^{s2} \quad k_4^{s2})$ are constant matrices and positive definite, and the switching function $\text{sgn}(s(t)_{4\times1})$ is a discontinuous function, which can be given as follows [29]:

$$\text{sgn}(s(t)_i) = \begin{cases} \dfrac{s(t)_i}{\|s(t)_i\|}, & \text{when} \quad \|s(t)_i\| > 0 \\ 0 & \text{when} \quad \|s(t)_i\| = 0 \end{cases} \tag{11}$$

According to (9) and (10), the following equation is obtained:

$$\begin{aligned} \dot{s}(t)_{4\times1} &= \ddot{q}_d + \Lambda_{4\times4}\dot{e}_w(t)_{4\times1} - M_0^{-1}(q)u(t) + H_0(q)\dot{q} \\ &= -k_{4\times4}^{s1} s(t)_{4\times1} - k_{4\times4}^{s2}\,\text{sgn}(s(t)_{4\times1}) \end{aligned} \tag{12}$$

Above all, the SMC controller based on reaching law can be expressed as follows:

$$u(t)_{4\times1} = M_0(q)(k_{4\times4}^{s1} s(t)_{4\times1} + k_{4\times4}^{s2}\,\text{sgn}(s(t)_{4\times1}) + \Lambda_{4\times4}(\dot{q}_d - \dot{q}) + \ddot{q}_d + H_0(q)\dot{q}) \tag{13}$$

where the switching function is used to improve the robustness of the system, but it will also cause undesired chattering and the chattering may cause high-frequency control input. Moreover, to improve the robustness of the system with uncertainties and decrease the chattering produced by the switching function, the ANN based adaptive law is introduced.

3.2. *Neural network adaptive law*

Many parameters in the dynamic system are difficult to measure accurately, and the existence of external disturbances makes it difficult to get a precise mathematical model. In this paper, RBF neural network is utilized to emulate the uncertain nonlinear function by creating an adaptive control law. Figure 5 shows a multi-input multi-output (MIMO) RBF neural network structure, which consists of three layer network structures, i.e., the input layer, hidden layer and output layer. There are 7 neurons employed in the hidden layer of this paper.

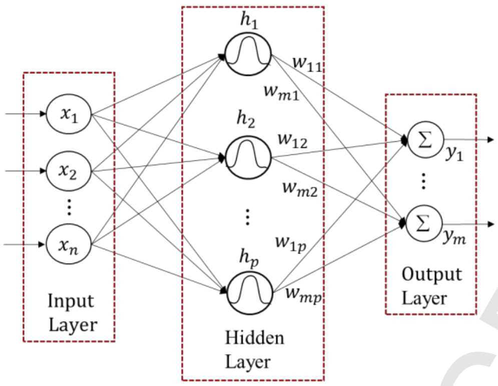

Fig.5 MIMO RBF neural network structure

In the case of the mathematical model with uncertainty $g(q)$, the sliding mode control law is obtained as follows:

$$\begin{aligned} u(t)_{4\times1} &= M_0(q)(k^{s1}_{4\times4}s(t)_{4\times1} + k^{s2}_{4\times4}\,\mathrm{sgn}(s(t)_{4\times1}) + \Lambda_{4\times4}(\dot{q}_d - \dot{q}) + \ddot{q}_d + H_0(q)\dot{q} + g(q)) \\ &= M_0(q)(k^{s1}_{4\times4}s(t)_{4\times1} + k^{s2}_{4\times4}\,\mathrm{sgn}(s(t)_{4\times1}) + f(x_{in})_{4\times1}) \end{aligned} \tag{14}$$

where $f(x_{in})_{4\times1} = \Lambda_{4\times4}(\dot{q}_d - \dot{q}) + \ddot{q}_d + H_0(q)\dot{q} + g(q)$. The RBF neural network are employed as a universal approximator to emulate any real continuous function $f(x_{in})_{4\times1}$ with its optimal parameters, the form is as follows:

$$f(x_{in})_{4\times1} = W^{*T}h(x_{in}) + \varepsilon(x_{in}) \tag{15}$$

where $x_{in} = [x_1, x_2, \cdots, x_n]^T \in R^n$ is the input vector, $W^* \in R^{4\times p}$ represents a vector of optimal network weights, $h(x_{in}) = [h_1(x_{in}), h_2(x_{in}) \cdots h_p(x_{in})]^T \in R^p$ represents a vector of basis function and there are 7 neurons in the hidden layer of the network, that is $p = 7$, $\varepsilon(x_{in})$ is approximation error of the network, which is bounded with $\|\varepsilon(x_{in})\| \le \varepsilon_N$, and ε_N is an unknown positive constant. For RBF neural network, the basis function $h(x_{in})$ is a particular network architecture with the form of Gaussian functions as [17]:

$$h_j(x_{in}) = \exp\left[-\frac{(x_{in} - c_j)^T(x_{in} - c_j)}{2b_j^2}\right] \tag{16}$$

where c_j is the coordinate vector of the center point of the Gauss basis function of the j neuron of the hidden layer, b_j is the width of the center point of the Gauss basis function of the j neuron of the hidden layer.

In terms of this RBF neural network, the approximate value $\hat{f}(x_{in})_{4\times1}$ is applied to estimate the unknown nonlinear function $f(x_{in})_{4\times1}$. The function $\hat{f}(x_{in})_{4\times1}$ is designed as:

$$\hat{f}(x_{in})_{4\times1} = \hat{W}^T h(x_{in}) \tag{17}$$

where $\hat{W}^T \in R^{4\times p}$ represents an updated weight matrix, and the function approximation error is given as follows:

$$\begin{aligned} \tilde{f}(x_{in})_{4\times1} &= f(x_{in})_{4\times1} - \hat{f}(x_{in})_{4\times1} \\ &= W^{*T} h(x_{in}) + \varepsilon(x_{in}) - \hat{W}^T h(x_{in}) \\ &= \tilde{W}^T h(x_{in}) + \varepsilon(x_{in}) \end{aligned} \tag{18}$$

Using the approximation ability of RBF neural network, the NNASMC control law is obtained as follows:

$$u(t)_{4\times1} = M_0(q)(k^{s1}_{4\times4} s(t)_{4\times1} + k^{s2}_{4\times4}\,\mathrm{sgn}(s(t)_{4\times1}) + \hat{f}(x_{in})_{4\times1}) \tag{19}$$

It is need to construct an adjustment mechanism for eliminate the unknown nonlinear function $f(x_{in})_{4\times1}$, and the state inputs of RBF neural network is defined as:

$$x_{in} = [e_w(t)_{4\times1} \quad \dot{e}_w(t)_{4\times1} \quad q \quad \dot{q}]^T \tag{20}$$

4. Stability analysis

Theorem 1: Consider the dynamic model of the omnidirectional mobile vehicle based on Mecanum wheel with uncertainties and external disturbances, as shown in Eq. (5). The proposed neural network adaptive sliding mode control (NNASMC) Eq. (19), if the weight of neural network is updated according to Eq. (21), then the stability of the closed-loop system can be guaranteed and the tracking error will converge to zero vector asymptotically.

$$\dot{\hat{W}} = \Gamma h(x_{in}) s^T(t)_{4\times1} \tag{21}$$

Proof: Let the Lyapunov function candidate be defined as

$$L = \frac{1}{2} s^T(t)_{4\times1} s(t)_{4\times1} + \frac{1}{2} tr(\tilde{W}^T \Gamma^{-1} \tilde{W}) \tag{22}$$

where Γ^{-1} is a positive-definite matrix, and $tr(\bullet)$ is the trace operator.

The derivative of Lyapunov function L along to time as:

$$\dot{L} = s^T(t)_{4\times1} \dot{s}(t)_{4\times1} + tr(\tilde{W}^T \Gamma^{-1} \dot{\tilde{W}}) \tag{23}$$

Substitute Eq. (9) into the Eq. (23), one can get:

$$\begin{aligned}\dot{L} &= s^T(t)_{4\times1}\dot{s}(t)_{4\times1} + tr(\tilde{W}^T\Gamma^{-1}\dot{\tilde{W}}) \\ &= s^T(t)_{4\times1}[\ddot{e}_w(t)_{4\times1} + \Lambda_{4\times4}\dot{e}_w(t)_{4\times1}] + tr(\tilde{W}^T\Gamma^{-1}\dot{\tilde{W}}) \\ &= s^T(t)_{4\times1}[\Lambda_{4\times4}\dot{e}_w(t)_{4\times1} + \ddot{q}_d - \ddot{q}] + tr(\tilde{W}^T\Gamma^{-1}\dot{\tilde{W}})\end{aligned} \tag{24}$$

Substitute Eq. (6) into the Eq. (24), we yields:

$$\begin{aligned}\dot{L} &= s^T(t)_{4\times1}[\Lambda_{4\times4}\dot{e}_w(t)_{4\times1} + \ddot{q}_d - \ddot{q}] + tr(\tilde{W}^T\Gamma^{-1}\dot{\tilde{W}}) \\ &= s^T(t)_{4\times1}\{\Lambda_{4\times4}\dot{e}_w(t)_{4\times1} + \ddot{q}_d \\ &\quad -[M_0^{-1}(q)u(t) - M_0^{-1}(q)E(q) - H_0(q)\dot{q}]\} + tr(\tilde{W}^T\Gamma^{-1}\dot{\tilde{W}}) \\ &= s^T(t)_{4\times1}[\Lambda_{4\times4}\dot{e}_w(t)_{4\times1} + \ddot{q}_d + g(q) + H_0(q)\dot{q} \\ &\quad - M_0^{-1}(q)u(t)] + tr(\tilde{W}^T\Gamma^{-1}\dot{\tilde{W}}) \\ &= s^T(t)_{4\times1}[f(x_{in})_{4\times1} - M_0^{-1}(q)u(t)] + tr(\tilde{W}^T\Gamma^{-1}\dot{\tilde{W}})\end{aligned} \tag{25}$$

Inserting Eq. (18) and Eq. (19) into the Eq. (25), we have:

$$\begin{aligned}\dot{L} &= s^T(t)_{4\times1}[f(x_{in})_{4\times1} - M_0^{-1}(q)u(t)] + tr(\tilde{W}^T\Gamma^{-1}\dot{\tilde{W}}) \\ &= s^T(t)_{4\times1}\{f(x_{in})_{4\times1} - M_0^{-1}(q)[M_0(q)(k^{s1}_{4\times4}s(t)_{4\times1} \\ &\quad + k^{s2}_{4\times4}\,\mathrm{sgn}(s(t)_{4\times1}) + \hat{f}(x_{in})_{4\times1})]\} + tr(\tilde{W}^T\Gamma^{-1}\dot{\tilde{W}}) \\ &= s^T(t)_{4\times1}(f(x_{in})_{4\times1} - \hat{f}(x_{in})_{4\times1} - k^{s1}_{4\times4}s(t)_{4\times1} \\ &\quad - k^{s2}_{4\times4}\,\mathrm{sgn}(s(t)_{4\times1})) + tr(\tilde{W}^T\Gamma^{-1}\dot{\tilde{W}}) \\ &= s^T(t)_{4\times1}(\tilde{f}(x_{in})_{4\times1} - k^{s1}_{4\times4}s(t)_{4\times1} - k^{s2}_{4\times4}\,\mathrm{sgn}(s(t)_{4\times1})) \\ &\quad + tr(\tilde{W}^T\Gamma^{-1}\dot{\tilde{W}}) \\ &= s^T(t)_{4\times1}(\tilde{W}^T h(x_{in}) + \varepsilon(x_{in}) - k^{s1}_{4\times4}s(t)_{4\times1} - k^{s2}_{4\times4}\,\mathrm{sgn}(s(t)_{4\times1})) \\ &\quad + tr(\tilde{W}^T\Gamma^{-1}\dot{\tilde{W}}) \\ &= s^T(t)_{4\times1}(\varepsilon(x_{in}) - k^{s1}_{4\times4}s(t)_{4\times1} - k^{s2}_{4\times4}\,\mathrm{sgn}(s(t)_{4\times1})) \\ &\quad + tr\tilde{W}^T(\Gamma^{-1}\dot{\tilde{W}} + h(x_{in})s^T(t)_{4\times1})\end{aligned} \tag{26}$$

where $k^{s1}_{4\times4}, k^{s2}_{4\times4}$ are positive definite matrices and $\dot{\tilde{W}} = \dot{W}^* - \dot{\hat{W}}$. W^* is a constant and represents a vector of optimal network weights and $\hat{W}$ is a variable and represents an updated weight matrix, hence $\dot{\tilde{W}} = -\dot{\hat{W}}$. Therefore, $\dot{L}$ can be expressed as follows:

$$\begin{aligned}\dot{L} &= s^T(t)_{4\times1}(\varepsilon(x_{in}) - k_{4\times4}^{s1}s(t)_{4\times1} - k_{4\times4}^{s2}\operatorname{sgn}(s(t)_{4\times1})) \\ &\quad + tr\tilde{W}^T(\Gamma^{-1}\dot{\tilde{W}} + h(x_{in})s^T) \\ &= s^T(t)_{4\times1}\varepsilon(x_{in}) - (k_{4\times4}^{s1}s^T(t)_{4\times1}s(t)_{4\times1} + k_{4\times4}^{s2}\|s(t)_{4\times1}\|) \\ &\quad + tr\tilde{W}^T(-\Gamma^{-1}\dot{\hat{W}} + h(x_{in})s^T(t)_{4\times1})\end{aligned} \tag{27}$$

We define $\dot{L}_1 = s^T(t)_{4\times1}\varepsilon(x_{in}) - (k_{4\times4}^{s1}s^T(t)_{4\times1}s(t)_{4\times1} + k_{4\times4}^{s2}\|s(t)_{4\times1}\|)$, where $\|\varepsilon(x_{in})\| \le \varepsilon_N$, $k_{4\times4}^{s1}s^T(t)_{4\times1}s(t)_{4\times1} \ge 0$, and we assume $k_{4\times4}^{s2}$ satisfies $k_{4\times4}^{s2} > \varepsilon_N$, thus, we get:

$$\begin{aligned}\dot{L}_1 &\le \|\varepsilon(x_{in})\| s^T(t)_{4\times1} - (k_{4\times4}^{s1}s^T(t)_{4\times1}s(t)_{4\times1} + k_{4\times4}^{s2}\|s(t)_{4\times1}\|) \\ &\le \varepsilon_N\|s(t)_{4\times1}\| - k_{4\times4}^{s2}\|s(t)_{4\times1}\| - k_{4\times4}^{s1}s^T(t)_{4\times1}s(t)_{4\times1} \le 0\end{aligned} \tag{28}$$

With the adaptive control law Eq. (21) and the inequality of Eq. (28), the function of $\dot{L}$ is derived as:

$$\begin{aligned}\dot{L} &= s^T(t)_{4\times1}\varepsilon(x_{in}) - (k_{4\times4}^{s1}s^T(t)_{4\times1}s(t)_{4\times1} + k_{4\times4}^{s2}\|s(t)_{4\times1}\|) \\ &\quad + tr\tilde{W}^T(-\Gamma^{-1}\dot{\hat{W}} + h(x_{in})s^T(t)_{4\times1}) \\ &= s^T(t)_{4\times1}\varepsilon(x_{in}) - (k_{4\times4}^{s1}s^T(t)_{4\times1}s(t)_{4\times1} + k_{4\times4}^{s2}\|s(t)_{4\times1}\|) \\ &\le \varepsilon_N\|s(t)_{4\times1}\| - k_{4\times4}^{s2}\|s(t)_{4\times1}\| - k_{4\times4}^{s1}s^T(t)_{4\times1}s(t)_{4\times1} \le 0\end{aligned} \tag{29}$$

Therefore, according to Lyapunov stability theorem the closed-loop system is asymptotically stable, and the tracking errors will converge to zero set within a finite time, which means the sliding surface is asymptotically stable.

5. Simulation Results

In order to illustrate the effectiveness of the proposed control scheme, two simulations for trajectory tracking of the omnidirectional mobile vehicle are performed in MATLAB/Simulink environment. In addition, the performance of the NNASMC control method are compared with the SMC control method and conventional PID control method, and we consider the uncertainties and external disturbances of the model in the simulations. The neural networks include 7 neurons and the parameters of the control scheme that proposed in this paper are selected as: $k_{4\times4}^{s1} = diag(15\quad 15\quad 15\quad 15)$, $k_{4\times4}^{s2} = diag(10\quad 10\quad 10\quad 10)$, $\Lambda_{4\times4} = diag(15\quad 15\quad 15\quad 15)$, $b = 10$,

$$c = \begin{bmatrix} -1.5 & -1 & -0.5 & 0 & 0.5 & 1 & 1.5 \\ -1.5 & -1 & -0.5 & 0 & 0.5 & 1 & 1.5 \\ -1.5 & -1 & -0.5 & 0 & 0.5 & 1 & 1.5 \\ -1.5 & -1 & -0.5 & 0 & 0.5 & 1 & 1.5 \end{bmatrix}.$$

The physical parameters of MWOV are listed in Table I.

Table I Physical parameters of the vehicle

No.	Symbol	Parameter	Unit	Value
1	m	Mass of the vehicle	kg	1[illegible]7
2	R	Wheel radius	m	0.[illegible]76
3	W	Width of the platform	m	0.25
4	L	Length of the platform	m	0.225
5	I_z	Inertia of the vehicle	$kg \cdot m^2$	0.32
6	I_ω	Inertia of the wheel	$kg \cdot m^2$	0.029
7	D_w^0	Coefficient of the wheel	—	0.4

A. Case 1: S shape curve trajectory

The equation of the S shape curve trajectory is given as:

$$\begin{cases} x = t \\ y = \sin(0.5x) + 0.5x + 1 \\ \varphi_{r\omega} = 0 \end{cases}$$

where t is the simulation time in seconds and satisfies $t \geq 0$. The initial posture of the mobile vehicle is $\begin{bmatrix} x & y & \varphi_\omega \end{bmatrix}^T = \begin{bmatrix} 0 & 0 & 0 \end{bmatrix}^T$. To verify the efficient and effective properties of the control scheme that proposed this paper for MWOV with uncertainties and external disturbances, robustness tests have been done in the simulation experiment. The external disturbances in the dynamic model τ_d is given by $\tau_d = 20\begin{bmatrix} \sin(t) & \sin(t) & \sin(t) & \sin(t) \end{bmatrix}^T$, and the uncertainties is acting on the system during the simulation experiment at t=15s, which lasts for 2s. The uncertainties is taken as follows:

$$\delta(t) = \begin{cases} 0.2\sin(t) & 15 \leq t \leq 17 \\ 0 & \text{otherwise} \end{cases}$$

The S shape curve trajectory tracking results of the experiment with traditional PID controller, SMC controller and NNASMC controller in x-y plane is presented in Fig. 6. The tracking performance along x and y directions are shown in Fig.7 (a) and (b), respectively, and Fig.7(c) presents the rotation angle tracking result of the vehicle. It can be seen that in Fig.6 and Fig.7 the performance of the proposed approach is better than that of the SMC approach and traditional PID control method with the system under effects of uncertainties and external disturbances. When the uncertainties are fed from 15s to 17s, NNASMC has better robustness and trajectory tracking performance. In Fig.8 the tracking errors of the three applied control methods in the three coordinate directions are shown. It is observed from Fig.8 that the proposed control scheme has smaller tracking error, faster convergence rate and higher tracking precision than the other two control method applied in this paper. In Fig.9 the speed of MWOV and angular velocity of four wheels are shown.

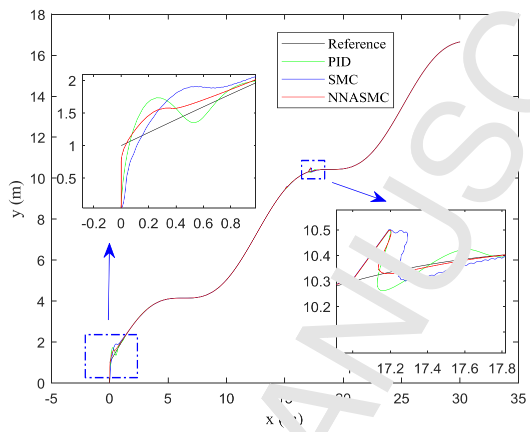

Fig.6 S shape curve trajectory tracking ability of the PID, SMC, and NNASMC in x–y plane

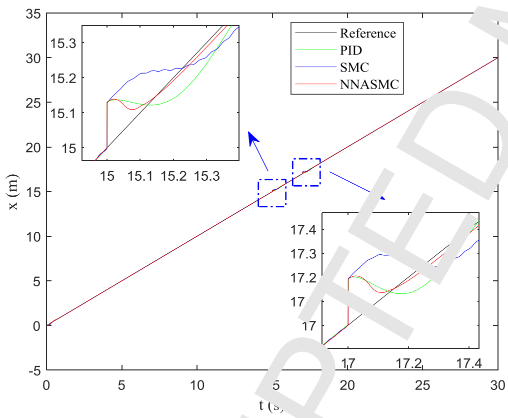

(a)

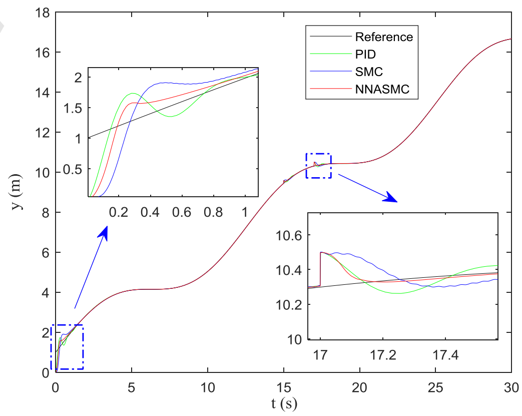

(b)

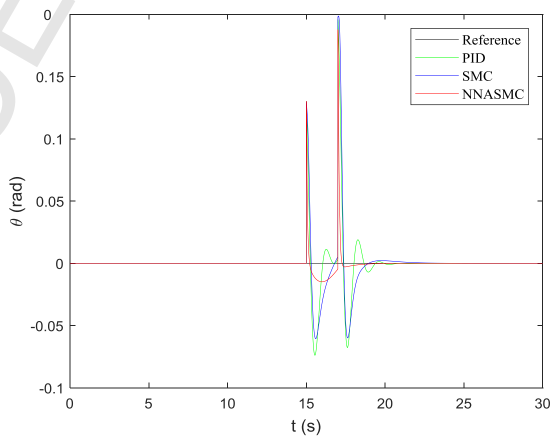

(c)

Fig.7 Trajectory tracking results in different directions. (a) Trajectory tracking in x-coordinate. (b) Trajectory tracking in y-coordinate. (c) Trajectory tracking of rotation angle.

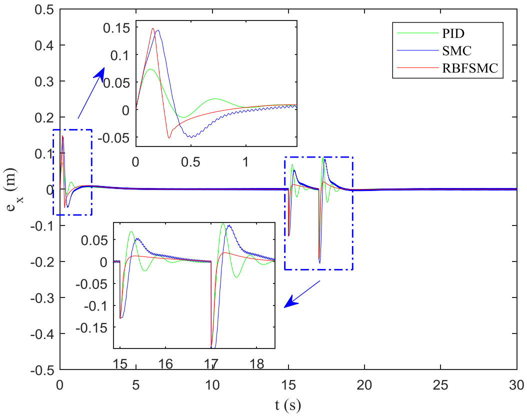

(a)

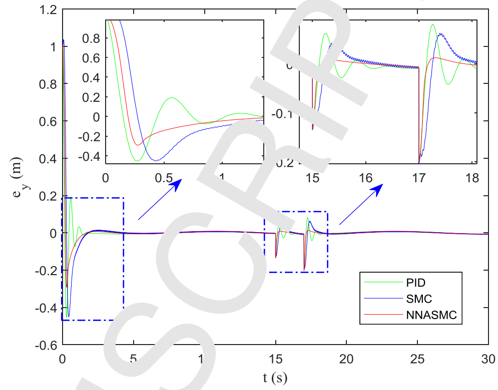

(b)

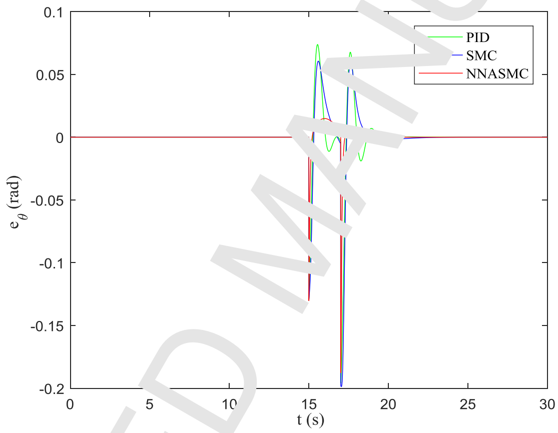

(c)

Fig.8 Trajectory tracking error in different directions. (a) Trajectory tracking error in x-coordinate. (b) Trajectory tracking error in y-coordinate. (c) Trajectory tracking error of rotation angle.

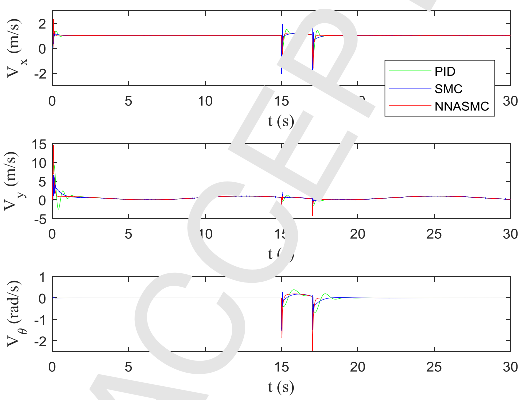

(a)

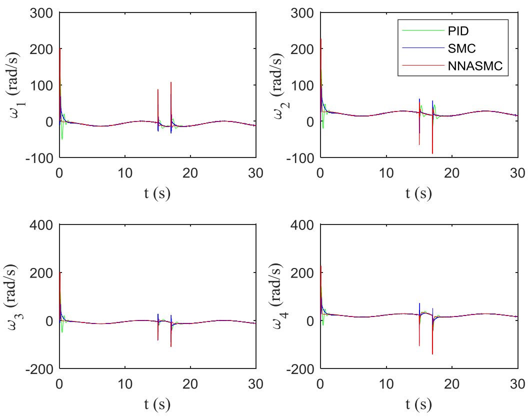

(b)

Fig.9 (a) Trajectory curve in x-coordinate, y-coordinate and rotation angle curve respectively. (b) Angular velocity of four wheels.

B. Case 2: Lemniscate trajectory

The equation of the Lemniscate trajectory is given as:

$$\begin{cases} x = 2\sin(0.25t) \\ y = 2\sin(0.5t) \\ \varphi_{\omega} = 0 \end{cases}$$

where t is the simulation time in seconds and satisfies $t \geq 0$. The initial posture of the mobile vehicle is $\begin{bmatrix} x & y & \varphi_{\omega} \end{bmatrix}^T = \begin{bmatrix} 0 & 1 & 0 \end{bmatrix}^T$. Like case 1, we also added external disturbances and uncertainties to the system in the experiment, and the external disturbances in the dynamic model τ_d is the same as case 1. The uncertainties is given as follows:

$$\delta(t) = \begin{cases} \frac{1}{\sqrt{2\pi}\sigma} e^{-\frac{t-\mu}{2\sigma^2}} + 0.2\sin(t) & 14 \leq t \leq 18 \\ 0 & \text{otherwise} \end{cases}$$

where $\mu = 16, \sigma = 1$, and the uncertainties is acting on the system during the simulation experiment at t=14s, which lasts for 4s.

Figure 10 shown the lemniscate trajectory tracking results of the traditional PID controller, sliding mode controller and the proposed control scheme, and the tracking performance along x, y direction and the rotation angle tracking result are shown in Fig.11 (a) , (b) and (c), respectively. Form Fig.10 and Fig.11, it can be seen that NNASMC has better robustness and trajectory tracking performance compared to the other two controllers, especially when the system is subjected to uncertainties and unknown external disturbances. Moreover, in Figs. 12, the position tracking errors in the x, y directions and the rotation angle tracking error are shown. From position tracking error results, it is observed that the NNASMC has smaller tracking errors compared other two controllers with the system under the effect of model uncertainties and external disturbances. In Fig.13 the speed of MWOV and angular velocity of four wheels are shown.

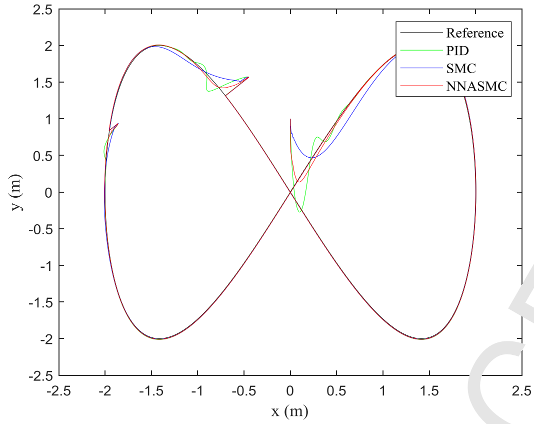

Fig.10 Lemniscate trajectory ability of the PID, SMC, and NNASMC in x–y plane

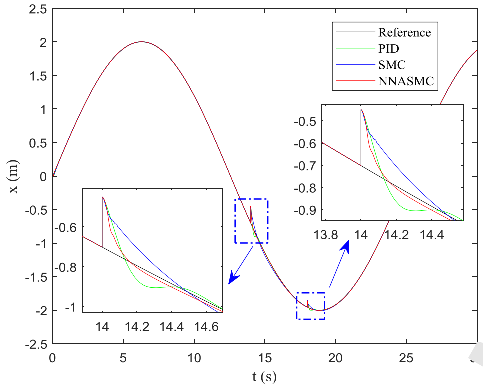

(a)

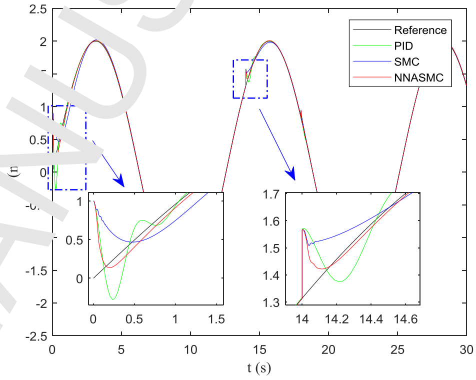

(b)

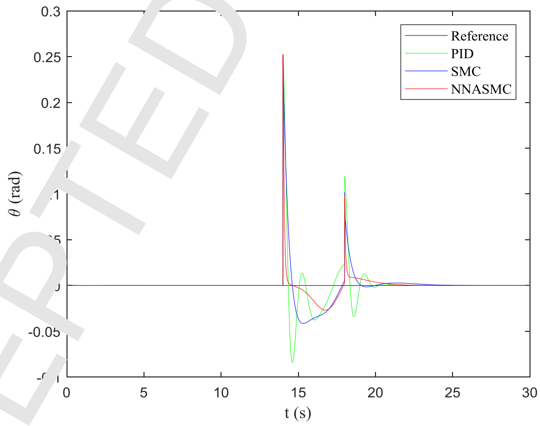

(c)

Fig.11 Trajectory tracking results in different directions. (a) Trajectory tracking in x-coordinate. (b) Trajectory tracking in y-coordinate. (c) Trajectory tracking of rotation angle.

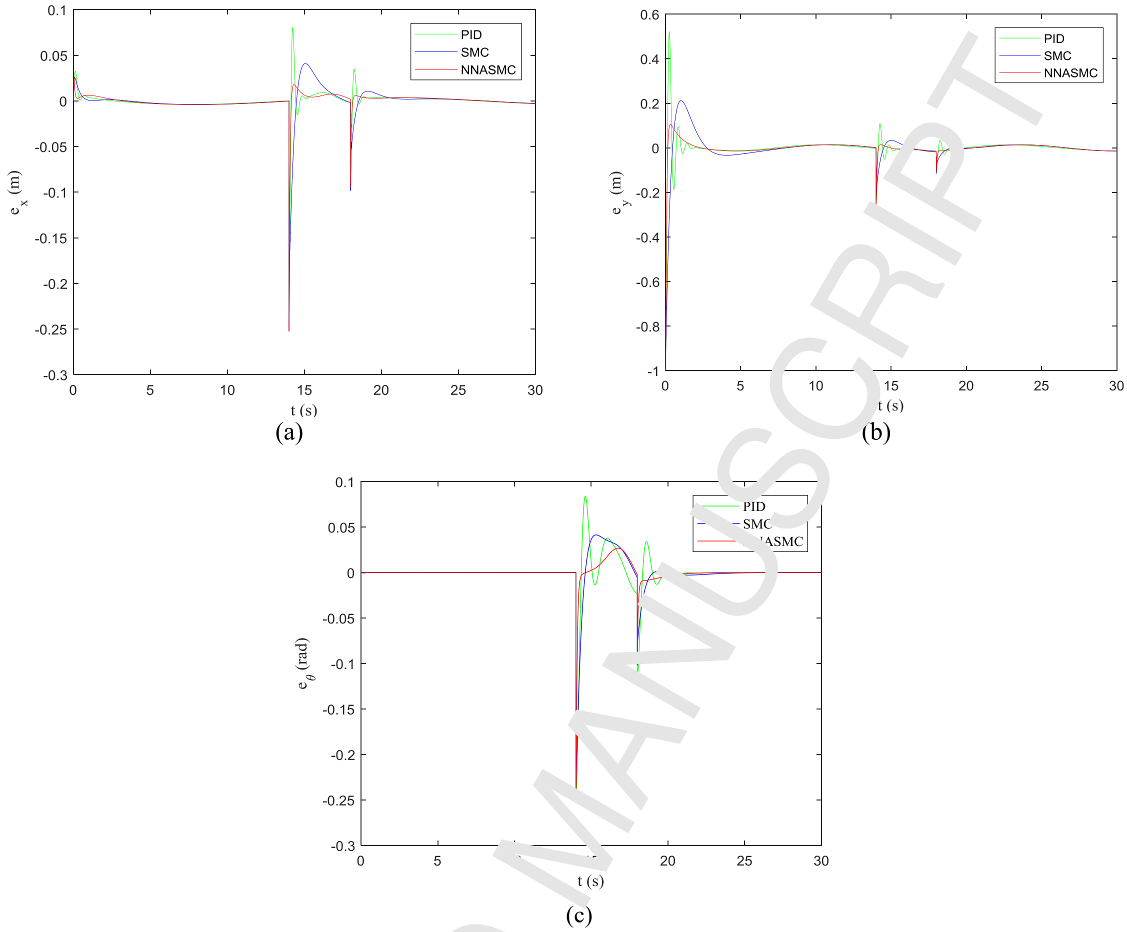

Fig.12 Trajectory tracking error in different directions. (a) Trajectory tracking error in x-coordinate. (b) Trajectory tracking error in y-coordinate. (c) Trajectory tracking error of rotation angle.

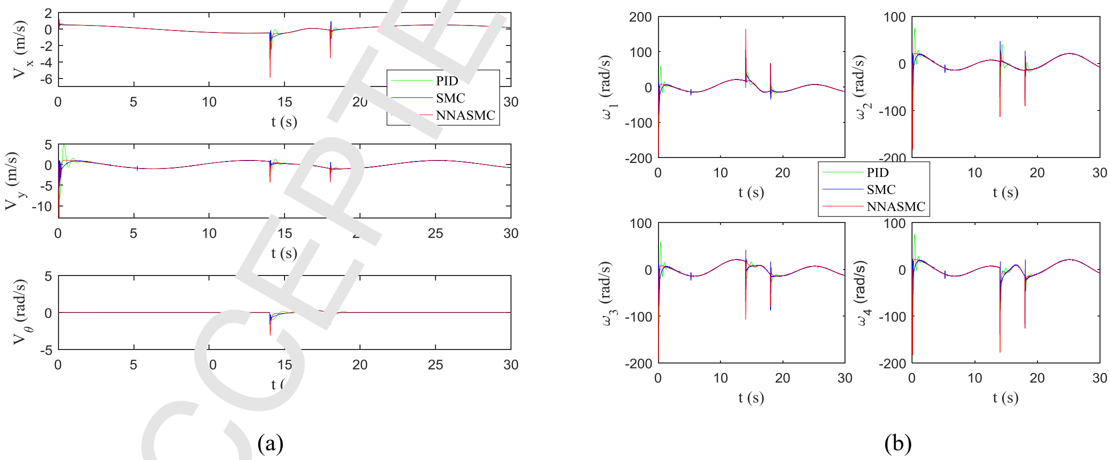

Fig.13 (a) Trajectory curve in x-coordinate, y-coordinate and rotation angle curve respectively. (b) Angular velocity of four wheels.

From these simulation results, it can be concluded that the NNASMC control scheme has better robust capability including the shorter convergence time and smaller tracking error. These simulation results also reflect the adaptability of NNASMC control approach which makes the closed-loop control system have much better adaptive ability for the four Mecanum wheels omnidirectional mobile vehicle dynamic system in presence of uncertainties and external disturbances. Therefore, the NNASMC control law is effective and feasible for tracking control of MWOV with uncertainties and unknown external disturbances.

6. Experiments

To verify the efficacy of the NNASMC controller, we realize this system on an actual MWOV as shown in Fig. 14. A real-time control system has been implemented by using the Robot Operating System (ROS). There are two computers has been adopted, the computer with Linux 14.04 system has the specification as, Intel Core-i5 CPU 2.60 GHz and 4 GB RAM and the computer with Windows 10 system has the specification as, Intel Core-i5 CPU 3.30 GHz and 4 GB RAM. The experimental setup and the Block diagram of ROS MATLAB/Simulink experiment scheme is shown in Fig. 14.

During real-time implementation the ode45 (Dormand-Prince) solver available in MATLAB/Simulink 2017b is used to solve the equation. Matlab Robot Operating System Toolbox is utilized to develop an interface between ROS and MATLAB/Simulink 2017b. When the run is started, the two computers send and receive data in the form of messages in ROS to compose a closed loop system.

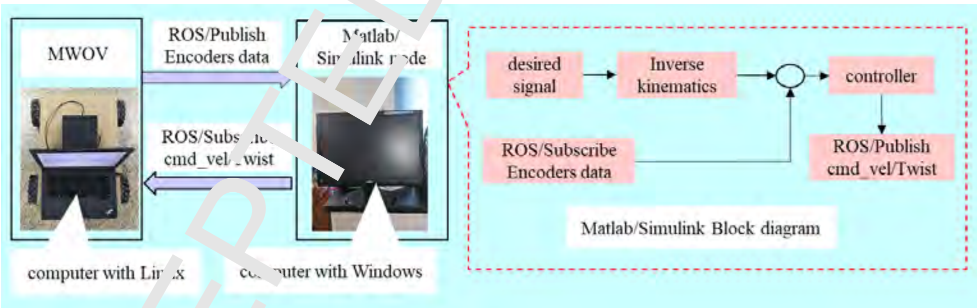

Fig.14. Experimental setup and block diagram of the experiment scheme

In order to prove the supremacy of the proposed controller over SMC and PID, two experiments are conducted and the results is shown in Fig. 15 and Fig. 16. The speed of MWOV in x, y direction and rotation speed as the desired signal of MATLAB/Simulink node. In the result figures, the black line represents reference signal, the green line represents the signal with PID controller, the blue line represents the signal with SMC controller and the red line represents the signal with NNASMC controller.

A. Experiment 1: Rectangle trajectory

The rectangle trajectory is chosen as desired trajectory, and the dimensions of the trajectory are 2 m in length and 2 m in width. The rectangle trajectory curves in x–y plane are shown in Fig. 15(a), the tracking performance along x and y direction and rotation angle tracking results are shown in Fig. 15(b), the velocity along x and y direction and rotation angular velocity results are shown in Fig. 15(c), the line speed curve of four wheels are shown in Fig. 15(d) and the real motion experiment environment is shown in Fig. 15(e).

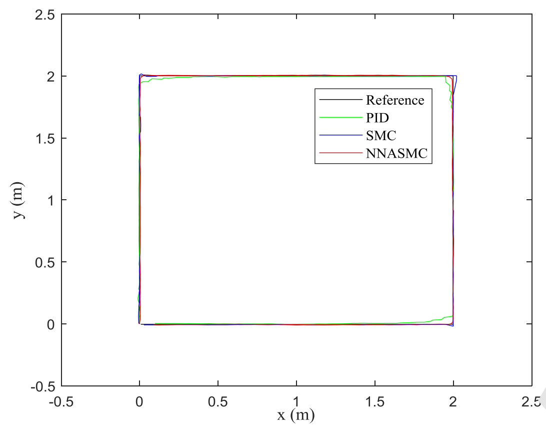

(a)

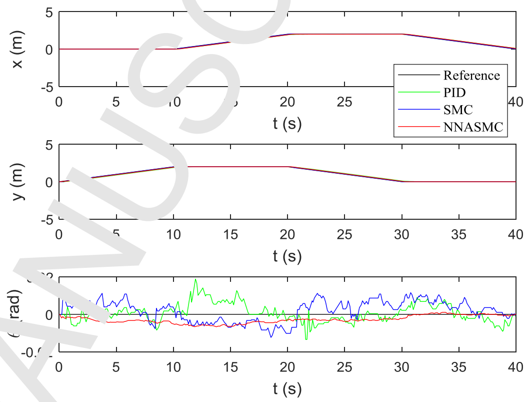

(b)

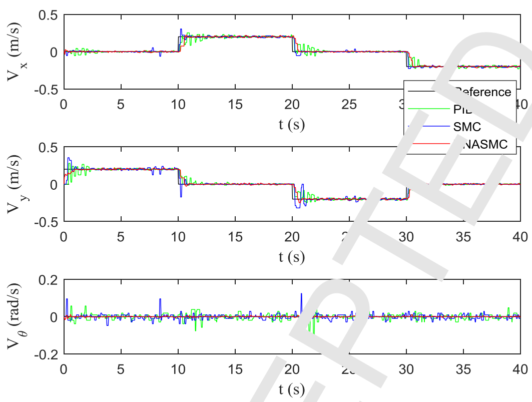

(c)

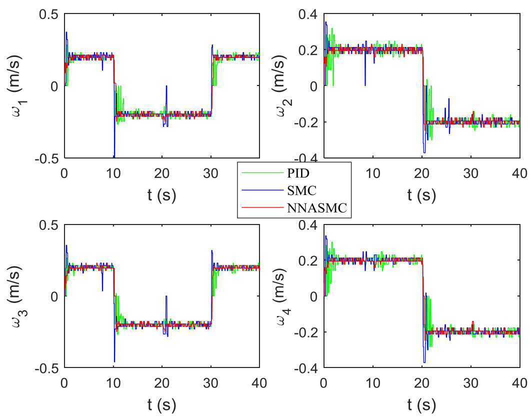

(d)

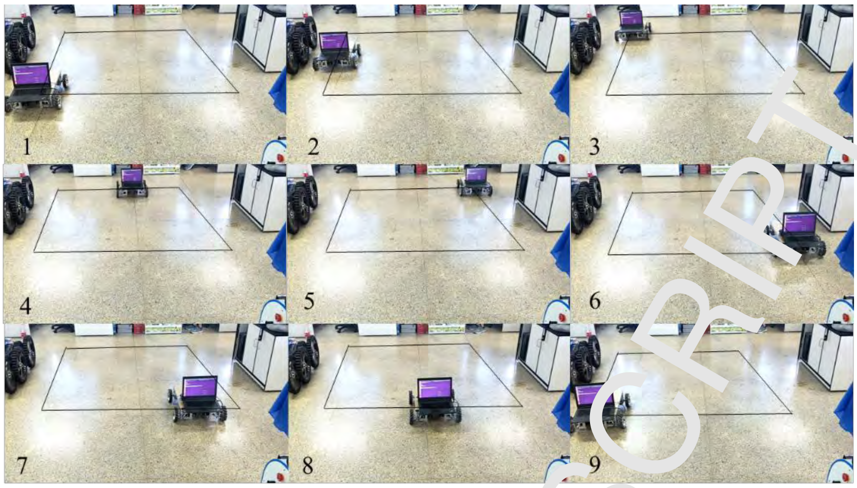

(e)

Fig.15 Experimental results. (a) Trajectory curve in x–y plane. (b) Trajectory curve in x-coordinate, y-coordinate and rotation angle curve respectively. (c) The speed curve in x-coordinate, y-coordinate and rotation speed curve respectively. (d) Line speed of four wheels. (e)Real motion experiment environment.

B. Experiment 2: Lemniscate trajectory

The Lemniscate trajectory is chosen as desired trajectory in this experiment. The trajectory tracking curves in x–y plane are shown in Fig. 16(a), the tracking performance along x and y direction and rotation angle tracking results are shown in Fig. 16(b), the velocity along x and y direction and rotation angular velocity results are shown in Fig. 16(c), the line speed carve of four wheels are shown in Fig. 16(d) and the real motion experiment environment is shown in Fig. 16(e).

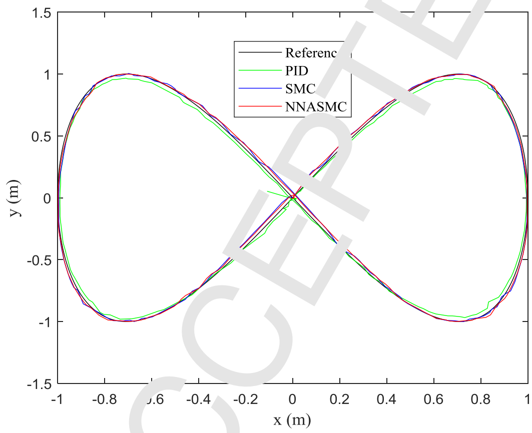

(a)

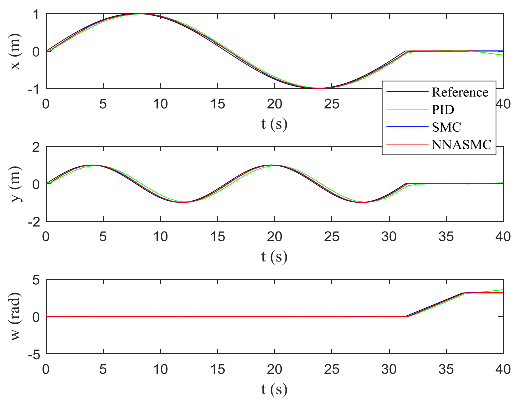

(b)

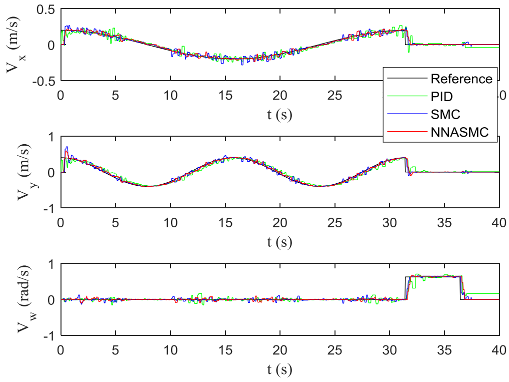

(c)

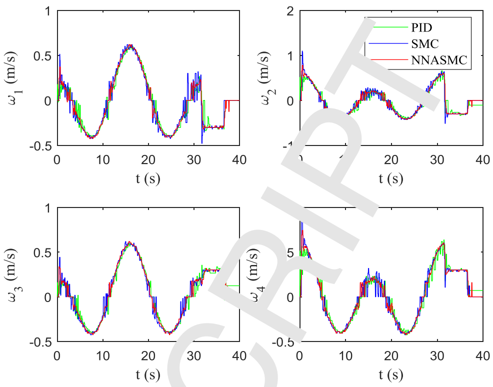

(d)

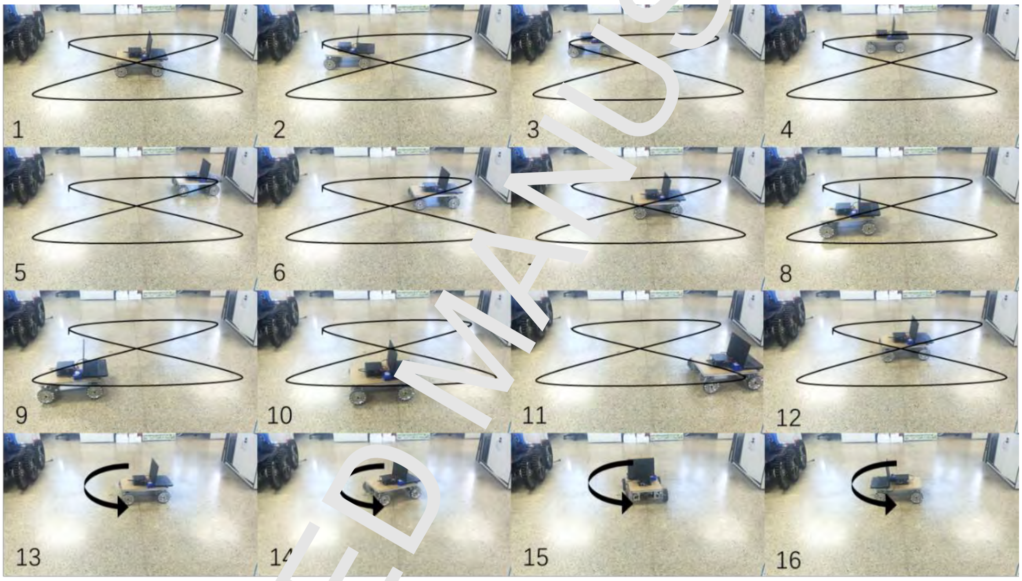

(e)

Fig.16 Experimental results. (a) Trajectory curve in x–y plane. (b) Trajectory curve in x-coordinate, y-coordinate and rotation angle curve respectively. (c) The speed curve in x-coordinate, y-coordinate and rotation speed curve respectively. (d) Line speed of four wheels. (e)Real motion experiment environment.

From the trajectory curve results of the two experiments, the NNASMC, SMC and PID control scheme are not much difference, the response trajectory curve have the same excellent quality. The efficacy of NNASMC can also be proved from the velocity curves, which show that the control system based on NNASMC controller has smaller trajectory tracking error and less chattering of linear velocity and angular velocity. The speed along x and y direction and rotation speed as shown in Fig.15(c) and Fig.16(c), the line speed of four wheels as shown in Fig.15(d) and Fig.16(d) illustrate that the proposed control scheme has better performance compared with SMC and PID controller.

7. Conclusion

In this paper, an ANN based adaptive SMC scheme is proposed for the MWOV in presence of uncertainties and external disturbances. The kinematic and dynamic models are established for the MWOV with uncertainties and external disturbances. To achieve the robustness of the control system, the SMC based dynamic controller is designed, while the ANN based adaptive law is introduced to model and estimate the various uncertainties disturbances. In addition, the PID controller is applied to the out-loop controller for the trajectory-tracking. According to the Lyapunov theory, the stability of the proposed NNASMC method is proved. The performance of the proposed NNASMC method is verified and compared with the classical PID and SMC methods through simulations and experiments on the omnidirectional vehicle. Results validate the effectiveness and robustness of the NNASMC method in presence of uncertainties and unknown external disturbances. In the following work, the study of autonomous obstacle avoidance in the process of trajectory tracking is under investigation.

Acknowledgments

This work is supported by National Natural Science Foundation of China (No. 61703012 and No. 81471770), Beijing Natural Science Foundation (No. 4182010), and BJUT Promotion Project on Intelligent Manufacturing under Grant (No. 040000546317552).

References

[1] B. Chu, Position compensation algorithm for omnidirectional mobile robots and its experimental evaluation, International Journal of Precision Engineering & Manufacturing, 2017, 18 (12):1755-1762.

[2] C. C. Tsai, H. L. Wu, F, C. Tai, and Y.S. Chen, Distributed consensus formation control with collision and obstacle avoidanceforuncertain networked omnidirectional multi-robot systems using fuzzy wavelet neural networks, International Journal of Fuzzy Systems, 2016, 19 (5):1-17.

[3] V. Alakshendra, and S. S. Chiddarwar, Simultaneous balancing and trajectory tracking control for an omnidirectional mobile robot with a cylinder using switching between two robust controllers, International Journal of Advanced Robotic Systems, 2017, 14(6): 1-16.

[4] N. Tlale, and M. Villiers, Kinematics and dynamics modelling of a Mecanum wheeled mobile platform, in Proceedings of 15th International Conference on Mechatronics and Machine Vision in Practice, 2008: 657-662.

[5] K. Zimmermann, I. Zeidis, and M. Abdelrahman, Dynamics of mechanical systems with Mecanum wheels, Springer International Publishing, 2014: 269-279.

[6] P.F. Muir, and C.P. Neuman, Kinematic modeling for feedback control of an omnidirectional wheeled mobile robot, IEEE International Conference on Robotics & Automation, 1990, 4:1772-1778.

[7] Y. Tian, S. Zhang, J. Liu, F. Chen, L. Li, and B. Xia. Research on a new omnidirectional mobile platform with heavy loading and flexible motion, Advances in Mechanical Engineering, 2017, 9 (9): 168781401772668.

[8] J. Kang, B. Kim, and M. Chung, Development of omnidirectional mobile robots with Mecanum wheels assisting the disabled in a factory environment, in Proceedings of 8th International Conference on Control, Automation and Systems, 2008: 2070-2075.
[9] K. Tu, and S. Luo, Design and implementation of omni-directiona1 soccer robots for RoboCup, in Proceedings of 2006 IEEE International Conference on Systems, 2006: 2000–2005.
[10] J. Kim, S. Woo, J. Kim, J. Do, S. Kim, and S. Bae, Inertial navigation system for an automatic guided vehicle with Mecanum wheels, International Journal of Precision Engineering & Manufacturing, 2012, 13 (3):379-386.
[11] V. Alakshendra, and S. S. Chiddarwar, Adaptive robust control of Mecanum-wheeled mobile robot with uncertainties, Nonlinear Dynamics, 2017, 87 (4): 2147-2169.
[12] C.C. Tsai, H.L. Wu, F.C. Tai, and Y.S. Chen. Adaptive backstepping decentralized formation control using fuzzy wavelet neural networks for uncertain mecanum-wheeled omnidirectional multi-vehicles, IEEE International Conference on Industrial Technology IEEE, 2016:1446-1451.
[13] C. Y. Chen, T. H. S. Li, Y. C. Yeh, and C. C. Chang, Design and implementation of an adaptive sliding-mode dynamic controller for wheeled mobile robots, Mechatronics, 2009, 19 (2):156-166.
[14] B. Miao, T. Li, W. Luo, A DSC and MLP based robust adaptive NN tracking control for underwater vehicle, Neurocomputing, 2013, 111 (6):184-189.
[15] M. S. Kim, J.H. Shin, S.G. Hong, and J.J. Lee, Designing a robust adaptive dynamic controller for nonholonomic mobile robots under modeling uncertainty and disturbances, Mechatronics, 2003, 13 (5): 507-519.
[16] O. Purwin, and R. D. Andrea, Trajectory generation and control for four wheeled omnidirectional vehicles, Robotics & Autonomous Systems, 2006, 54 (1): 13-22.
[17] M. Yue, L. Wang, and T. Ma, Neural network based terminal sliding mode control for WMRs affected by an augmented ground friction with slippage effect, IEEE/CAA Journal of Automatica Sinica, 2017, 4 (3):498-506.
[18] C. C. Tsai, and H. L. Wu, Nonsingular terminal sliding control using fuzzy wavelet networks for Mecanum wheeled omni-directional vehicles, IEEE International Conference on Fuzzy Systems, 2010:1-6.
[19] C. L. Hwang, and H. M. Wu, Trajectory tracking of a mobile robot with frictions and uncertainties using hierarchical sliding-mode under-actuated control, Iet Control Theory & Applications, 2013, 7 (7):952-965.
[20] H. Ashrafiuon, K. R. Muske, L. C. McNinch, and R. A. Soltan, Sliding-mode tracking control of surface vessels, IEEE Transactions on Industrial Electronics, 2008, 55 (11): 4004-4012.
[21] D. Qian, C. Li, S. G. Lee, and C. Ma, Robust formation maneuvers through sliding mode for multi-agent systems with uncertainties, IEEE/CAA Journal of Automatica Sinica, 2018, 5(1): 342-351.
[22] A. Ferrara, and G. P. Incremona, Design of an integral suboptimal second-order sliding mode controller for the robust motion control of robot manipulators, IEEE Transactions on Control Systems Technology, 2015, 23 (6): 2316-2325.
[23] V. T. Yen, Y. N. Wang, N. V. Cuong, N. X. Quynh, and V. H. Thich, Robust adaptive sliding mode control for industrial robot manipulator using fuzzy wavelet neural networks, International Journal of Control Automation & Systems, 2017, 15(6):2930-2941.
[24] N. B. Hoang, H. J. Kang, Neural network-based adaptive tracking control of mobile robots in the presence of wheel slip and external disturbance force. Neurocomputing, 2016, 188:12-22.
[25] C. Y. Chen, T. H. S. Li, Y. C. Yeh, and C. C. Chang, Design and implementation of an adaptive sliding-mode dynamic controller for wheeled mobile robots, Mechatronics, 2009, 19 (2):156-166.
[26] J. T. Huang, T. V. Hung, and M. L. Tseng, Smooth switching robust adaptive control for omnidirectional mobile robots, IEEE Transactions on Control Systems Technology, 2015, 23(5): 1986-1993.
[27] C. Yang, X. Wang, L. Cheng, and H. Ma, Neural-learning-based telerobot control with guaranteed performance, IEEE Transactions on Cybernetics, 2016, 47 (10): 3148-3159.
[28] Y. Wang, and D. Chang, Motion performance analysis and layout selection for motion system with four Mecanum wheels, Journal of Mechanical Engineering, 2009, 45(5):307-308.

[29] Y. Jia, X. Song, and S. Xu, Modeling and motion analysis of four-Mecanum wheel omni-directional mobile platform, in Proceedings of 2014 Automatic Control Conference, 2014: 328-333.
[30] J. Niu, Q. Yang, X. Wang, and R. Song, Sliding mode tracking control of a wire-driven upper-limb rehabilitation robot with nonlinear disturbance observer, Frontiers in Neurology, 2017, 8:1-10.